

## On-line commissioning of SHIPTRAP

S. Rahaman<sup>a</sup>, M. Block<sup>b,\*</sup>, D. Ackermann<sup>b</sup>, D. Beck<sup>b</sup>, A. Chaudhuri<sup>b,c</sup>, S. Eliseev<sup>b,d</sup>,  
H. Geissel<sup>b,e</sup>, D. Habs<sup>f</sup>, F. Herfurth<sup>b</sup>, F.P. Heßberger<sup>b</sup>, S. Hofmann<sup>b</sup>, G. Marx<sup>c</sup>,  
M. Mukherjee<sup>g</sup>, J.B. Neumayr<sup>f</sup>, M. Petrick<sup>e</sup>, W.R. Plaß<sup>e</sup>, W. Quint<sup>b</sup>, C. Rauth<sup>b</sup>,  
D. Rodríguez<sup>h</sup>, C. Scheidenberger<sup>b,e</sup>, L. Schweikhard<sup>c</sup>, P.G. Thirolf<sup>f</sup>, C. Weber<sup>b,i</sup>

<sup>a</sup> University of Jyväskylä, P.O. Box 35 (YFL), 40014 Jyväskylä, Finland

<sup>b</sup> Gesellschaft für Schwerionenforschung, Planckstrasse 1, 64291 Darmstadt, Germany

<sup>c</sup> Ernst-Moritz-Arndt-Universität, Domstrasse 10a, 17489 Greifswald, Germany

<sup>d</sup> PNPI RAS, Gatchina, Leningrad District 188300, Russia

<sup>e</sup> Justus-Liebig-Universität, Heinrich-Buff-Ring 16, 35392 Gießen, Germany

<sup>f</sup> Ludwig-Maximilians-Universität, Am Coulombwall 1, 85748 Garching, Germany

<sup>g</sup> Universität Innsbruck, Technikerstr. 25, 6020 Innsbruck, Austria

<sup>h</sup> LPC, ENSICAEN, 6 Bd. Marechal Juin, 14050 Caen Cedex, France

<sup>i</sup> Johannes-Gutenberg-Universität, Staudingerweg 7, 55099 Mainz, Germany

Received 27 December 2005; received in revised form 15 January 2006; accepted 19 January 2006

Available online 13 March 2006

This paper is dedicated to Jürgen Kluge on the occasion of his 65th birthday.

### Abstract

The on-line commissioning of the Penning-trap mass spectrometer SHIPTRAP was successfully completed with a mass measurement of holmium and erbium radionuclides produced at SHIP. A large fraction of contaminant ions created in the stopping cell was identified to originate from the buffer-gas supply system. Using a liquid nitrogen cold trap they were reduced to a tolerable amount and mass measurements of <sup>147</sup>Er, <sup>148</sup>Er, and <sup>147</sup>Ho with relative uncertainties of about  $1 \times 10^{-6}$  were performed.

© 2006 Elsevier B.V. All rights reserved.

PACS: 07.75.+h Mass spectrometers; 21.10.Dr Binding energies and masses

Keywords: Atomic mass; Binding energy; Penning trap; Erbium; Holmium

### 1. Introduction

The Penning-trap mass spectrometer SHIPTRAP [1] at GSI Darmstadt was set up for precision mass measurements of heavy radionuclides produced in fusion-evaporation reactions and separated by the velocity filter SHIP [2]. This approach offers the unique possibility to access the region of elements heavier than uranium which are not available at ISOL or fragmentation facilities. In this region at present still many masses are only known from extrapolations of systematic trends [3]. From mass measurements the nuclear binding energy can be deduced and hence

systematic studies along isotopic or isotonic chains provide information about the nuclear shell structure in that region. The main challenge for the elements heavier than uranium is the very low production rate, dropping to only a few ions per week in the extreme case of  $Z = 112$ .

A schematic drawing of the SHIPTRAP setup is shown in Fig. 1. The reaction products from SHIP with energies in the order of about 100–500 keV/u are stopped in a gas-filled stopping cell with an overall efficiency, including the extraction radiofrequency quadrupole (RFQ), of about 5–8% as described in [4]. To improve the quality of the ion beam extracted from the stopping cell and for an efficient injection into the Penning-trap system an RFQ cooler and buncher is utilized. In this buffer-gas-filled RFQ the ions are cooled within a few milliseconds and extracted as a low-emittance bunched beam. Ions from the stopping cell

\* Corresponding author.

E-mail address: [m.block@gsi.de](mailto:m.block@gsi.de) (M. Block).

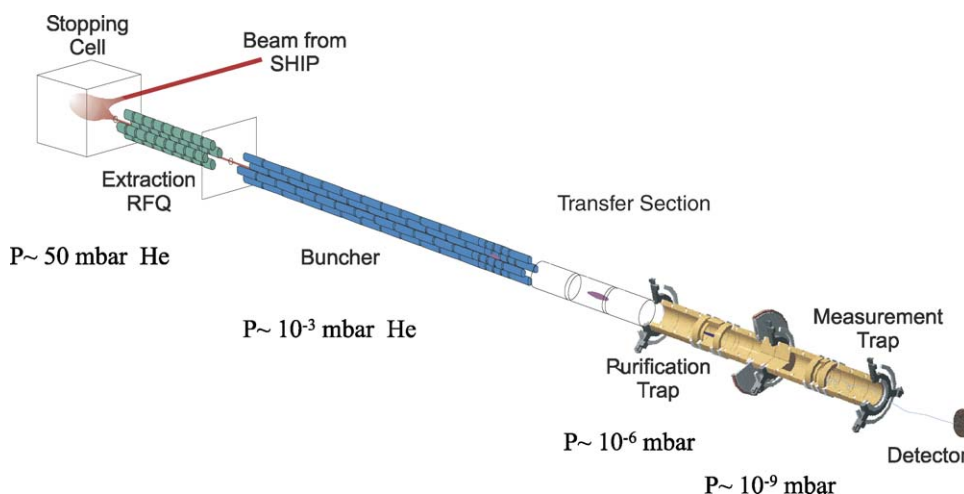


Fig. 1. Schematic overview of the SHIPTRAP facility.

can optionally be stacked in the RFQ. A system of two cylindrical Penning traps in one superconducting magnet of 7 T field strength allows for high-precision mass measurements. The first trap with a mass resolving power of about 85,000 for  $^{133}\text{Cs}$  ions is used for isobaric purification. In the second trap mass measurements are performed by the time-of-flight ion cyclotron resonance (TOF-ICR) method [5]. A mass resolving power of  $10^6$  is routinely achieved. This allows to resolve isomeric states with an excitation energy on the order of 100 keV in the region  $A \sim 150$ . If an unresolved isomeric state is present, an average mass of the isomeric pair is obtained in the experiment. An unambiguous mass determination of the ground state is then only possible if the excitation energies and production ratios of the involved states are known.

Extensive off-line tests were carried out in order to characterize each component individually. In addition, on-line experiments at GSI and at the Maier–Leibnitz Laboratory in Garching were performed with radioactive and stable ions in order to optimize the stopping process in the gas cell [4]. In this paper the last stage of commissioning of the complete system in a beam time in July 2004, resulting in first mass measurements of radioactive ions at SHIPTRAP, is described. It was the final step in the process of bringing SHIPTRAP into operation.

Two major difficulties occurred during this run and the successful measurement became a real challenge: A surprisingly high background of impurity ions mainly created in the stopping cell was observed. Furthermore, as found after the run, the micro-channel plate detector was not working properly, resulting in a reduced detection efficiency of only about 2% compared to about 50% for normal operation. Nonetheless, the separation of the radioactive isobars  $^{147}\text{Ho}$  and  $^{147}\text{Er}$  in the purification trap was demonstrated and first mass measurements were possible.

## 2. Production of the radionuclides and stopping in the buffer-gas cell

The radionuclides of interest were produced in the reaction  $^{92}\text{Mo}(^{58}\text{Ni}, \text{xpy})$  at SHIP with a primary beam energy of 4.36 MeV/u. Under these conditions the cross-section of the

most abundant nuclide  $^{147}\text{Ho}$  was on the order of 50 mbarn. A rotating target wheel with an average target thickness of  $616 \mu\text{g}/\text{cm}^2$  made of 97% enriched  $^{92}\text{Mo}$  was used. A typical total production rate of a few 100 kHz for a primary beam intensity of 100 particle nA was expected from calculations predicting a yield of about 30 kHz for  $^{147}\text{Ho}$ . Since SHIP is a velocity filter a cocktail beam of different reaction products from the different evaporation channels was delivered to SHIPTRAP.

The mean energy of the reaction products was  $75 \text{ MeV} \pm 10\%$  after SHIP taking into account the energy loss in the target and an additional thin carbon foil used to equilibrate the charge state distribution. To match this energy to the energy acceptance of the gas cell, which was operated at 47 mbar, a  $7.1 \mu\text{m}$  thick titanium foil with a diameter of 80 mm was used as entrance window. The gas cell was baked prior to operation at  $150^\circ\text{C}$  for 24 h. The buffer gas was ultra-pure helium (purity 99.9999%) supplied via a commercial gas purifier (SAES Mono Torr) keeping impurities on a ppb level.

The stopping efficiency in the buffer-gas cell is limited due to the range straggling for the given energy spread of the incident ion beam. From calculations a value of up to 20% is expected for the chosen reaction. The stopped ions were extracted from the gas cell utilizing an RF funnel operated at 800 kHz with an amplitude of 160 V and an axial drift field between 5 and 10 V/cm. The ions extracted from the stopping cell were transversally cooled in the extraction RFQ at a pressure of about  $10^{-2}$  mbar. The extraction RFQ was operated at an RF frequency of 1 MHz with an amplitude of 250 V. The ions were injected into the RFQ cooler and buncher where they were further cooled transversally and longitudinally and finally extracted as bunches of a few  $\mu\text{s}$  width. The RFQ buncher was operated at a buffer-gas pressure of  $5 \times 10^{-3}$  mbar at an RF frequency of 1 MHz with an amplitude of 200 V.

## 3. Identification of the ions extracted from the stopping cell

The ejected bunches were transferred to the purification Penning trap where they were stored and further cooled. Since the

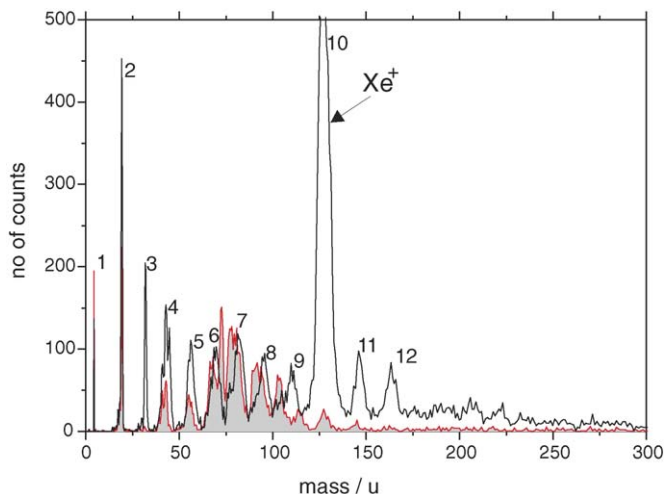


Fig. 2. Time-of-flight mass spectrum of ions extracted from the purification trap. The ions were trapped for about 400 ms. The mass assignment is based on a calibration with  $^{133}\text{Cs}^+$  ions. The black spectrum was recorded before, the grey shaded spectrum after a cold trap in the gas supply line was activated. Peak 10 contains xenon and the ions of interest are contained in peak 11 corresponding to  $m = 147(2)$ . Table 1 lists some species which were tentatively assigned to the other peaks.

trapping volume of the purification trap is rather large, it could be loaded in such a way that ions of different mass were captured simultaneously. The ions were trapped for about 400 ms, axially cooled in collisions with the buffer-gas atoms and ejected. They were detected on a micro-channel plate detector behind the magnet. From their time of flight the mass of the ions extracted from the stopping cell can be obtained with an uncertainty of about 2 u. The mass of the ions was determined relative to the time of flight of  $^{133}\text{Cs}^+$  reference ions applying the relation:

$$\frac{T_1}{T_2} = \sqrt{\frac{m_1}{m_2}}, \quad (1)$$

where  $T_1$  and  $T_2$  denote the time of flight of mass  $m_1$  and  $m_2$ , respectively. A mass spectrum obtained in this way is shown in Fig. 2. A surprisingly high number of contaminant ions over a wide mass range was observed. The mass range corresponding to each peak and possible species tentatively assigned to it are listed in Table 1.

The detected impurity ions include water clusters, hydrocarbons and noble gases even though the gas cell was baked. The strongest contamination (peak no. 10 of the black curve) was identified as xenon which was additionally confirmed by a cyclotron frequency measurement of the most abundant xenon isotopes in the purification trap. The ions of interest were contained in peak 11 corresponding to  $m = 147(2)$ . The peak at  $m = 164$  might contain molecular ions formed by a reaction of the ions of interest with water. Under these unfavorable conditions with a large number of impurities a measurement was hardly possible. Even if the ions of interest could still be selected, the efficiency was reduced by charge exchange and molecule formation in the gas cell and by space charge effects in the buncher.

Since xenon was the most prominent contaminant, it was concluded that the impurities were originating from the buffer gas

Table 1  
Ion species tentatively assigned to the mass spectrum shown in Fig. 2

Peak	Mass	Possible species
1	4	$\text{He}^+$
2	19(1)	$\text{H}_2\text{O}^+$ , $\text{H}_3\text{O}^+$
3	31(2)	$\text{O}_2^+$
4	44(2)	$\text{CO}^+$ , $\text{C}_2\text{H}_3\text{O}^+$
5	55(2)	$(3\text{H}_2\text{O} + \text{H})^+$
6	68(2)	$(\text{O}_2 + 2\text{H}_2\text{O})^+$
7	84(2)	$^{84}\text{Kr}^+$
8	95(2)	?
9	110(2)	$6\text{H}_2\text{O}^+$
10	129(3)	$^{129-132}\text{Xe}^+$
11	147(2)	$^{147}\text{Ho}^+$ , $^{147}\text{Er}^+$
12	164(2)	$(^{147}\text{Ho} + \text{H}_2\text{O})^+$ , $(^{147}\text{Er} + \text{H}_2\text{O})^+$

The identification is based on the time of flight from the purification trap to the MCP detector.  $^{129,132}\text{Xe}^+$ ,  $^{147}\text{Er}^+$  and  $^{147}\text{Ho}^+$  were also identified by their cyclotron frequencies determined from a cooling resonance in the purification trap.

supply line. By activating a liquid nitrogen cold trap situated in the gas feeding line close to the stopping cell they were reduced substantially as shown in Fig. 2. In the figure mass spectra of ions extracted from the gas cell before and after (grey shaded) activating the cold trap are shown. Both spectra were accumulated over the same time interval so the peak height can be directly compared.

The xenon peak and the peaks of heavier contaminants disappeared almost completely. Some of the low-mass impurities such as water were at least reduced, while other peaks such as helium were almost unchanged. Hence it was confirmed that xenon was mainly introduced by the gas supply system. Since the intensity of peak 11 around mass 147 decreased as well with the cold trap in operation, it also contained contamination in addition to the holmium and erbium isotopes, probably  $(\text{Xe} + \text{H}_2\text{O})^+$ . The peak for helium was unaffected since the helium was created in the trap region in a discharge. The ratio of impurities to ions of interest dropped to about 100 with the cold trap in operation, a ratio that could be handled in the purification trap.

#### 4. Isobaric selection and mass measurement in the purification trap

With the conditions after activating the cold trap the buffer-gas cooling with RF excitation [6] in the purification trap was applied to select a particular isobar at  $A = 147$ . A time-of-flight spectrum of ions ejected from the purification trap recorded during a scan of the cyclotron excitation frequency at  $A = 147$  around holmium and erbium is shown in Fig. 3. In this accumulated time-of-flight spectrum the low-mass contaminants helium and water were observed besides the peak at mass 147. They were created in an unwanted electrical discharge during the entire trapping time, i.e., also after the magnetron excitation which drives unwanted ions out of the trap center, and could not be removed by the excitation scheme applied.

A cooling resonance, i.e., the number of extracted ions as a function of the RF excitation frequency, is shown in Fig. 4. The two isobars  $^{147}\text{Er}^+$  and  $^{147}\text{Ho}^+$  whose mass difference corresponds to a frequency difference of 49.5 Hz

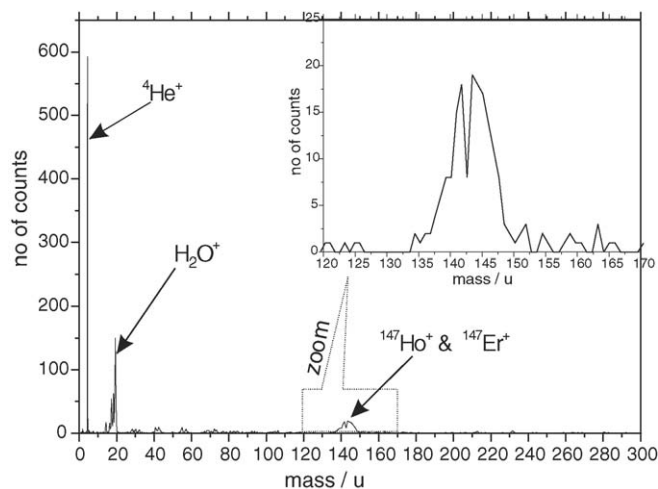


Fig. 3. Time-of-flight mass spectrum of ions ejected from the purification trap with the buffer-gas cooling applied to center  $^{147}\text{Ho}^+$  on the trap axis. The mass region around 147 is zoomed and shown as inset.

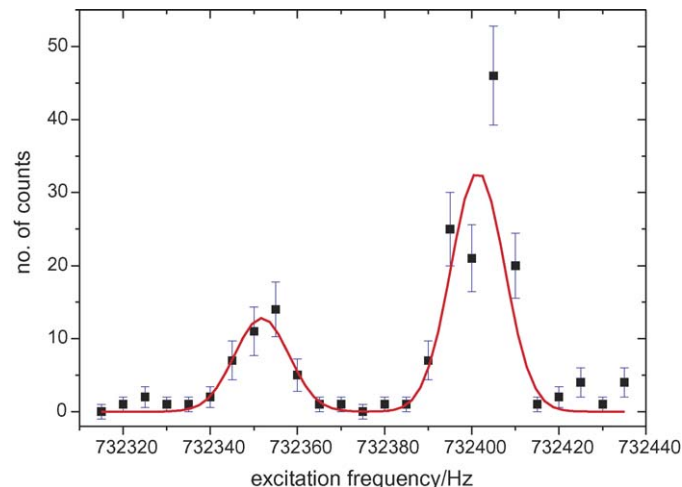


Fig. 4. Number of ions observed after ejection from the purification trap as a function of the cyclotron excitation frequency. A mass resolving power of about 60,000 was achieved for a total cycle time of 400 ms and a cyclotron excitation time of 200 ms.

were clearly resolved with a mass resolving power of about 60,000.

In general the buffer-gas cooling technique in the purification trap is only used to prepare cooled and isobarically purified samples for a subsequent mass measurement in the measurement trap using the time-of-flight ion cyclotron frequency (TOF-ICR) technique. However, since the cyclotron frequency of the ion can be determined from a cooling resonance as well, it can be used for a mass measurement if the magnetic field is calibrated

by a reference ion of known mass. This method is rarely used for a mass determination since the resolution is limited by the buffer gas. In addition, unwanted ions still present in the trap at a larger magnetron radius may affect the result even though possible frequency shifts are expected to be negligible on the achievable level of uncertainty.

To account for magnetic field changes, a cyclotron frequency measurement of the reference ion  $^{133}\text{Cs}^+$  was performed before and after the measurement of the ion of interest. The magnetic field at the actual time of the measurement was then obtained from a linear interpolation of the two calibration points. In all measurements parameters such as buffer-gas pressure, excitation times, and amplitudes for the magnetron and cyclotron excitation were kept constant.

The center frequency was obtained by fitting a Gaussian to the data points keeping the baseline fixed at zero counts. In the case of the holmium peak shown in Fig. 4 two data points in the maximum deviate from the fit curve by about two  $\sigma$ . This deviation is still in agreement with statistical fluctuations according to a  $\chi^2 = 1.8$  obtained for the displayed fit. Since the error bar of the point above the fit curve is larger than the one of the point below the fit curve, it influences the result of the fit less. If a different fit favoring the higher point is taken, a  $\chi^2 = 5.7$  is obtained, but the result for the center frequency is not changing. However, a different ratio between the number of  $^{147}\text{Ho}^+$  ions to the number of  $^{147}\text{Er}^+$  ions is obtained for the two different fits. It should reflect the production ratio of the two isobars which was expected to be about five from the cross-section calculations using the HIVAP code [7]. The displayed fit gives only a ratio of 2.5. However, the calculated cross-sections can be off by that factor. In addition, such a deviation may also occur due to a different chemical behavior leading to more losses by charge exchange or molecule formation for one of the nuclides.

The results of the mass measurement of  $^{147}\text{Er}$  and  $^{147}\text{Ho}$  in the purification trap are summarized in Table 2. The result of the experiment is the frequency ratio  $r = \nu_{\text{ref}}/\nu_c$  between the cyclotron frequency of the reference ion and the unknown ion. The atomic mass can then be calculated at any time using the most recent and hence most precise value of the reference mass available according to

$$m = r(m_{\text{ref}} - m_e) + m_e, \quad (2)$$

where  $m_e$  is the electron mass. The electron binding energy is negligible on the present level of uncertainty. In addition to the statistical uncertainty the uncertainty introduced by unobserved magnetic field changes was taken into account by adding the uncertainties quadratically. The latter one is on the order of  $5 \times 10^{-9}$  per hour.

Table 2

Results of the mass measurements of  $^{147}\text{Er}$  and  $^{147}\text{Ho}$  in the purification trap

Nuclide	$T_{1/2}(\text{s})$	Frequency ratio ( $r$ )	$N_{\text{total}}$	$m$ (u)	$\delta m/m$
$^{147}\text{Er}$	1.5	1.1056745(15)	66	146.95011(18)	$1.4 \times 10^{-6}$
$^{147}\text{Ho}$	5.8	1.1055997(11)	198	146.94017(13)	$0.9 \times 10^{-6}$

$r$  is the frequency ratio between the ion of interest and  $^{133}\text{Cs}$ ,  $N_{\text{total}}$  is the total number of detected ions,  $m$  is the atomic mass calculated according to Eq. (2),  $\delta m/m$  represents the relative mass uncertainty.

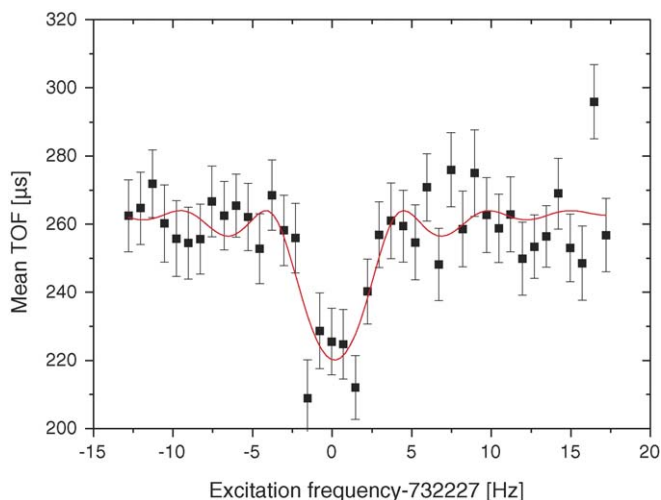


Fig. 5. Time-of-flight resonance of trapped  $^{147}\text{Ho}^+$  ions in the measurement trap for 200 ms cyclotron excitation time. The line shows a fit to the data points using the theoretically expected lineshape.

### 5. Mass measurements in the measurement trap by the TOF-ICR technique

For the nuclides  $^{147}\text{Ho}$  and  $^{148}\text{Er}$  mass measurements using the TOF-ICR technique in the measurement trap were performed. Due to low count rate of about 0.5 events/s at the MCP detector within a high background of impurities only a short measurement cycle with a cyclotron excitation time of 200 ms was used. For that excitation time only a precision comparable to the one obtained in the purification trap can be expected.

A time-of-flight cyclotron resonance obtained for  $^{147}\text{Ho}$  is shown in Fig. 5. About 2000 ions were accumulated for this resonance. The TOF contrast, defined as the relative time-of-flight difference between on and off-resonant ions, was low compared to the typical behavior obtained for resonances recorded with the reference ion. This is ascribed to the presence of impurity ions in the trap during the measurement which are not affected by the RF excitation. Hence their time of flight is longer than for the ions of interest resulting in an increased mean time of flight. Possible frequency shifts due to impurities were considered by a count rate class analysis as described in [8].

From TOF resonances as the one shown in Fig. 5 the cyclotron frequency for the ion of interest was obtained from fits of the theoretical lineshape to the data points. The magnetic field interpolation was performed in the same way as discussed above. A typical reference measurement took about 15 min, whereas a holmium or erbium resonance was recorded for about 1.5 h to accumulate the desired number of ions. The final result for the mass determination in the measurement trap is given in Table 3.

Table 3  
Results of the mass measurements of  $^{148}\text{Er}$  and  $^{147}\text{Ho}$  in the measurement trap

Nuclide	$T_{1/2}(\text{s})$	Frequency ratio ( $r$ )	$N_{\text{total}}$	$m$ (u)	$\delta m/m$
$^{148}\text{Er}$	4.6	1.1131594(17)	2965	147.94476(21)	$1.4 \times 10^{-6}$
$^{147}\text{Ho}$	5.8	1.1056003(18)	2269	146.94025(21)	$1.3 \times 10^{-6}$

$r$  is the frequency ratio between the ion of interest and  $^{133}\text{Cs}$  ions,  $N_{\text{total}}$  is the total number of detected ions,  $m$  is the atomic mass,  $\delta m/m$  represents the relative mass uncertainty.

The uncertainty includes in addition to the statistical one the uncertainty due to unobserved magnetic field changes as discussed in the previous section.

The relative uncertainty achieved for these measurements is on the order of  $10^{-6}$ , i.e., comparable to the results obtained from the purification trap measurements. This is not surprising since in both measurements the same cyclotron excitation time was used. The resolution achieved in the measurement trap was better by about a factor of two due to a better vacuum. However, the final uncertainty increased due to the extrapolation of the cyclotron frequency to one ion in the trap (cf. [8]) which was performed to consider contaminant ions. The result obtained for  $^{147}\text{Ho}$  is in agreement with the one obtained from the purification trap. For the first time a mass measurement of  $^{148}\text{Er}$  is presented here.

### 6. Compilation of results

The mass excess (ME) of the nuclides was calculated according to the equation

$$\text{ME} = (m[\text{in u}] - A)[\text{in keV}], \quad (3)$$

where  $A$  is the atomic mass number of the nucleus, and  $m$  is the atomic mass of the nucleus in u. The results of all measurements are summarized in Table 4. The mass of  $^{147}\text{Er}$  was experimentally determined for the first time with an uncertainty of 168 keV which is two times more precise than the extrapolated value of [3], but deviates from it by 586 keV. This deviation may be due to a long-lived isomeric state ( $11/2^-$ ) in  $^{147}\text{Er}$  with a half-life comparable to the one of the ground state ( $1/2^+$ ). According to [9] the excitation energy of the isomeric state is 100(50) keV corresponding to a frequency difference of about 1 Hz. This difference cannot be resolved in the purification trap. In the reaction both states will be produced. The state with the higher spin is expected to be more abundant but the exact ratio is unknown. Hence, the determined mass value is a combination of both states closer to the value of the isomeric state. In a future mass measurement in the measurement trap, using a long cyclotron excitation time to achieve a much higher resolving power, the situation should be clarified.

The result presented here for  $^{147}\text{Ho}$  with an uncertainty of 105 keV is in agreement with a previous measurement with a smaller uncertainty performed at the ESR storage ring [10] where  $\text{ME} = -55837(28)$  keV was obtained. The mass of  $^{148}\text{Er}$  was experimentally determined for the first time. The obtained value with an uncertainty of 198 keV agrees with the estimated values of [3].

Table 4  
Comparison of the mass values from the SHIPTRAP measurements of July 2004 to the atomic mass evaluation

Nuclide	ME <sub>exp</sub> (keV)	ME <sub>AME</sub> (keV)	ME <sub>exp</sub> – ME <sub>AME</sub> (keV)
<sup>147</sup> Er	–46464(168) <sup>a</sup>	–47050(300) <sup>b</sup>	586(344)
<sup>147</sup> Ho	–55729(122) <sup>a</sup>	–55837(28)	108(125)
<sup>148</sup> Er	–51454(198) <sup>c</sup>	–51650(200) <sup>b</sup>	196(281)
<sup>147</sup> Ho	–55647(204) <sup>c</sup>	–55837(28)	190(206)
<sup>147</sup> Ho	–55707(105)	–55837(28)	130(108)

ME<sub>exp</sub> represents the mass excess obtained from the measured cyclotron frequency ratio. ME<sub>AME</sub> are the AME values of [3]. In the last row the mean value of the two mass determinations for <sup>147</sup>Ho is given.

<sup>a</sup> The values obtained from the measurements in the purification trap.

<sup>b</sup> The values obtained from the measurement trap.

<sup>c</sup> Estimated AME values from extrapolations of systematic trends.

## 7. Conclusion

First on-line mass measurements of the rare-earth radionuclides <sup>147,148</sup>Er and <sup>147</sup>Ho were performed in July 2004 materializing the concept of SHIPTRAP. This first measurement suffered from problems with a large number of impurities created in the buffer-gas stopping cell and a detector with a reduced detection efficiency. Therefore, only a moderate uncertainty level was achieved. The masses of the two erbium isotopes were measured for the first time. For future experiments the cleanliness of the gas-stopping cell and the buffer-gas feeding system will be improved. In addition, a further increase of the overall efficiency of the system is required to access more exotic nuclides with lower production rates. This is expected from several technical improvements as for instance a new RF funnel in the buffer-gas cell for an increased extraction efficiency. A relative mass uncertainty on the order of  $\delta m/m = 5 \times 10^{-8}$  is expected in future measurements with the highest resolution and good statistics.

## Acknowledgements

Financial support by the EU (HPRI-CT-2001-50034) is gratefully acknowledged. We would like to thank Jürgen Kluge who

as pioneer of Penning-trap mass spectrometry at radioactive beam facilities established SHIPTRAP at GSI. We thank him for his patience, everlasting motivation, and continuous support also during the hard times of the project. His great experience was always a valuable asset from which we could benefit. SHIPTRAP has meanwhile started routine operation and we hope he will enjoy the great pleasures of a successful measurement program.

## References

- [1] J. Dilling, D. Ackermann, J. Bernard, F.P. Hessberger, S. Hofmann, W. Horiung, H.J. Kluge, E. Lamour, M. Maier, R. Mann, G. Marx, R.B. Moore, G. Münzenberg, W. Quint, D. Rodriguez, M. Schädel, J. Schönfelder, G. Sikler, C. Toader, L. Vermeeren, C. Weber, G. Bollen, O. Engels, D. Habs, P. Thirolf, H. Backe, A. Dretzke, W. Lauth, W. Ludolphs, M. Sewtz, *Hyperfine Interact.* 127 (2000) 491.
- [2] S. Hofmann, G. Münzenberg, *Rev. Mod. Phys.* 72 (2000) 733.
- [3] G. Audi, A.H. Wapstra, C. Thibault, *Nucl. Phys. A* 729 (2003) 337.
- [4] J.B. Neumayr, L. Beck, D. Habs, S. Heinz, J. Szerypo, P.G. Thirolf, V. Varantsov, F. Voit, D. Ackermann, D. Beck, M. Block, Z. Di, S.A. Eliseev, H. Geissel, F. Herfurth, F.P. Heßberger, S. Hofmann, H.-J. Kluge, M. Mukherjee, G. Münzenberg, M. Petrick, W. Quint, S. Rahaman, C. Rauth, D. Rodríguez, C. Scheidenberger, G. Sikler, Z. Wang, C. Weber, W.R. Plaß, M. Breitenfeldt, A. Chaudhuri, G. Marx, L. Schweikhard, A.F. Dodonov, Y. Novikov, M. Suhonen, *Nucl. Inst. Meth. B*, in press.
- [5] G. Gräff, H. Kalinowski, J. Traut, *Z. Phys. A* 297 (1980) 35.
- [6] G. Savard, St. Becker, G. Bollen, H.-J. Kluge, R.B. Moore, Th. Otto, L. Schweikhard, H. Stolzenberg, U. Wiess, *Phys. Lett. A* 158 (1991) 247.
- [7] W. Reisdorf, *Z. Phys. A* 300 (1981) 227.
- [8] A. Kellerbauer, K. Blaum, G. Bollen, F. Herfurth, H.-J. Kluge, M. Kuckein, E. Sauvan, C. Scheidenberger, L. Schweikhard, *Euro. Phys. J. D* 22 (2003) 53.
- [9] G. Audi, O. Bersillon, J. Blachot, A.H. Wapstra, *Nucl. Phys. A* 729 (2003) 3.
- [10] Yu.A. Litvinov, H. Geissel, T. Radon, F. Attallah, G. Audi, K. Beckert, F. Bosch, M. Falch, B. Franzke, M. Hausmann, M. Hellstrom, Th. Kerscher, O. Klepper, H.-J. Kluge, C. Kozhuharov, K.E.G. Lobner, G. Münzenberg, F. Nolden, Yu.N. Novikov, W. Quint, Z. Patykh, H. Reich, C. Scheidenberger, B. Schlitt, M. Steck, K. Summerer, L. Vermeeren, M. Winkler, Th. Winkler, H. Wollnik, *Nucl. Phys. A* 756 (1–2) (2005) 3.